Grid-aware aggregation and realtime disaggregation of distributed energy resources in radial networks

Nawaf Nazir* and Mads Almassalkhi*

***Abstract*— Dispatching a large fleet of distributed energy resources (DERs) in response to wholesale energy market or regional grid signals requires solving a challenging disaggregation problem when the DERs are located within a distribution network. This manuscript presents a computationally tractable convex inner approximation for the optimal power flow (OPF) problem that characterizes a feeders aggregate DERs hosting capacity and enables a realtime, grid-aware dispatch of DERs for radial distribution networks. The inner approximation is derived by considering convex envelopes on the nonlinear terms in the AC power flow equations. The resulting convex formulation is then used to derive provable nodal injection limits, such that any combination of DER dispatches within their respective nodal limits is guaranteed to be AC admissible. These nodal injection limits are then used to construct a realtime, open-loop control policy for dispatching DERs at each location in the network to collectively deliver grid services. The IEEE-37 distribution network is used to validate the technical results and highlight various use-cases.**

I. Introduction

The distribution system was engineered under the assumption that residential and commercial customers would only have power directed to them from the bulk grid. However, the increasing penetration of solar PV in distribution feeders has created so-called "prosumers" who (at times) can supply the grid with energy rather than just consume it. This leads to *reverse power flows* that can result in unexpected violations of voltage and transformer constraints, which may negatively impact system reliability [1]. Furthermore, the significant variability inherent to solar PV generation challenges traditional distribution system operating paradigms. Furthermore, with ubiquitous connectivity, smart appliances and DERs behind the meter (BTM) will soon underpin a demand that becomes inherently flexible. Many works in literature such as [2], [3] provide methodologies for aggregating the flexibility of DERs to provide grid services. The authors in [4] employ transactive energy principles as way to disaggregate flexibility amongst the individual DERs. However, none of these methods consider the underlying network, which may become overloaded when flexible demand is deployed at scale in the distribution network. The optimal power flow (OPF) represents an opportunity for algorithms to improve reliability and responsiveness of the grid and the dispatch of flexible resources (e.g., batteries, PV inverters). However, due to the sub-minutely timescale of the solar PV variability, these algorithms must be computationally tractable and, yet, representative of the physics. That is, grid optimization algorithms can ensure admissible network operations [5].

Since Carpentier's original OPF formulation [6] and subsequent improvements in optimization solvers, the OPF problem has become a powerful methodology for optimizing the dispatch of various grid resources. This is because OPF-based methods can account for the underlying grid physics, static network constraints on voltages and apparent branch flows, and resource limitations. However, it was also recognized early on that the nonlinear AC power flow equations that model the underlying grid physics render the AC OPF non-convex [7]. To overcome the computational challenges associated with non-convex AC network models, many recent techniques involve using linear or convex approximations [8]. Traditional optimization techniques for dispatching resources include linear OPF-based *LinDist* models [9]. These models work well close to the expected conditions of the system (e.g., low losses). In [10], it is shown how solutions of the *LinDist* model can lead to voltage violations under certain operating conditions. Similarly, the authors in [11] quantified the errors associated with more general linear power flow approximations. Recently, improved linear approximations of the power flow equations have been proposed that provide improved accuracy over a wider range of operation [12], [13]. However, the solution space of the AC power flow equations is highly non-convex, which means that such methods cannot guarantee network-admissible solutions under all net-load conditions.

Beyond linear approximations, recent attention in literature has focused on convex relaxations of the AC power flow equations, including second-order cone programs, semi-definite programs, and quadratic relaxations [14]. Several works in literature such as [15] have shown that, under certain analytical conditions, these relaxations can be exact and the solution of the relaxed convex problem then represents the global optimum of the original non-convex AC OPF problem. However, these conditions fail to hold under extreme solar PV injections when the network experiences reverse power flows, which engenders a non-zero duality gap solution that may not be network admissible, i.e., not

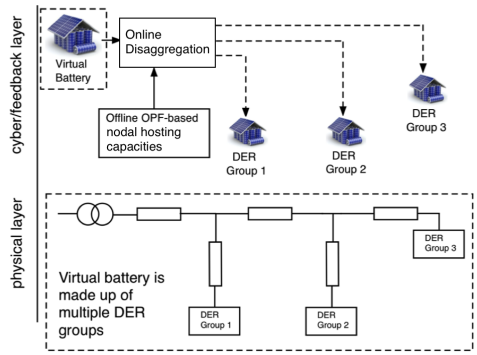

Fig. 1. A schematic representation of the network model. The physical layer represents the circuit that connects the different DER groups into an aggregate virtual battery, whereas the cyber layer represents the disaggregation of the virtual battery market signal to the DER groups based on the nodal hosting capacities that are determined offline. VB image source: https://esdnews.com.au/

*The authors are affiliated with the Department of Electrical and Biomedical Engineering, The University of Vermont, Burlington, VT 05405, USA. Support from U.S. Department of Energy award number DE-EE0008006 is gratefully acknowledged.

feasible in the original AC OPF formulation [16].

However, in many practical applications, guaranteeing network admissibility is more critical than finding the globally optimal solution. The authors in [17], develop an optimization-based method to certify whether a DER dispatch scheme can result in constraint violations. However, they do not discuss the network-admissible range of DER dispatch. The authors in [18] provide a convex restriction technique that guarantees an admissible solution, which they utilize in [19] to determine a feasible path from a known initial operating point to a desired final operating point. However, their method still requires coordination of DERs within the obtained convex restriction, whereas in our work, we aim to obtain a nodal range where DERs can operate independently In [20], the convex OPF formulation is based on an augmented second-order cone relaxation. The authors in [21] solve a large number of non-convex OPF problems to determine nodal injection bounds. However, these methods either rely on non-convex techniques or they cannot ensure that the full range of DER dispatch is network-admissible, which is the main focus herein.

The manuscript herein presents a novel convex approximation of the AC OPF problem to quantify the network-admissible range of DER nodal injections. In general, obtaining a convex inner approximation is NP-hard [22], however, the work herein uses the nonlinear branch-flow model (BFM) formulation of the AC power flow equations to define a convex envelope on the nonlinear terms relating the branch current, nodal voltages, and apparent power flows that is combined with the remaining linear relationships of the BFM to form a convex inner approximation. This convex inner approximation ensures that all feasible (and, hence, optimal) solutions in the convex OPF are also feasible in the non-convex AC OPF formulation. We denote such a solution as *network admissible* or *AC admissible*. From this approach, we achieve an OPF formulation that exhibits computational solve times similar to that of linear formulations with the added (and crucial benefit) that the formulation guarantees admissible solutions. This convex inner approximation is then utilized to determine the admissible DER dispatch ranges for nodes over a network, i.e., any combination of dispatching nodes across the network is admissible as long as each node is dispatched within its provided DER capacigy. This methodology represents a major shift in how to dispatch networked grid assets in distribution feeders and it overcomes practical limitations of methods that rely on repeatedly solving full, centralized AC OPFs at each time-step [23] or require extensive, realtime communication, grid data, and DER data [24]. The convex inner approximation methodology was first introduced in [25], but was utilized to optimize the reactive power set-points of controllable, discrete mechanical assets to maximize voltage margins (i.e., find a single optimal operating point). In this work, we have significantly extended the CIA approach to consider the admissible DER dispatch ranges. The main contributions of this manuscript are as follows:

- This manuscript improves over [25] to generalize a convex inner approximation of the AC OPF problem that is applicable to any radial, balanced distribution feeder, such as those with a mix of inductive and capacitive branches and with branch current and nodal voltage constraints.
- The generalized convex inner approximation (CIA) is employed to optimize the feeder's DER nodal capacities, which represent the ranges of admissible injections for DERs at each node in the network such that all branch flows and nodal voltages are within limits (i.e., network admissible). Thus, the optimized DER nodal capacities can then be trivially aggregated to form the network's range of admissible flexibility. Provable guarantees are provided for admissibility over the entire range of DER nodal dispatch.
- The CIA now generalizes admissibility to include guarantees on existence and uniqueness of the power flow solutions obtained through the optimized DER nodal capacities as a convex constraint. These conditions guarantee the existence of a solution to the non-linear power flow equations within the inner approximation.
- Simulation-based analysis assesses practicality of the proposed methods by investigating the conservativeness of the results and different reactive power strategies for enlarging a feeder's aggregate DER nodal capacity.
- The admissible DER nodal capacities are used within an open-loop, realtime disaggregation policy to account for network constraints while providing fast grid services.

The remainder of the manuscript is organized as follows. Section II develops the mathematical formulation of the convex inner approximation for the OPF problem using the robust bounds on nonlinear terms. Section III provides admissibility guarantees for the obtained DER nodal capacity and proposes an iterative algorithm that enlarges the admissible range. In Section IV, we present and analyze the effect of different nodal reactive power control policies to enlarge the range of admissible flexibility for the feeder, whereas Section V describes a realtime dispatch policy that disaggregates flexibility over a network in an admissible manner using the DER nodal capacity obtained through the convex inner approximation. Finally, section VI concludes the manuscript and lays out future research directions.

II. Formulating the Convex Inner Approximation

The nonlinear *DistFlow* model is often used to represent the underlying physics for a radial, balanced AC distribution network [9]. However, embedding this model within an AC OPF setting results in a non-convex formulation due to the nonlinear equations that map branch currents to branch power flows and nodal voltages. Common techniques that employ linear or convex relaxations are only valid under certain technical assumptions or near a pre-defined operating point. In this section, we develop a novel convex inner approximation of the AC OPF that is used to compute the range of allowable nodal net injections, such that any combination of nodal injections within those ranges are guaranteed to satisfy AC limits for voltages and branch flows.

A. Mathematical model

Consider a balanced, radial distribution network, shown in Fig. 2, as an undirected graph $\mathcal{G} = \{\mathcal{N} \cup \{0\}, \mathcal{L}\}$ consisting of a set of $N+1$ nodes with $\mathcal{N} := \{1,...,N\}$ and a set of N branches $\mathcal{L} := \{1,...,N\} \subseteq \mathcal{N} \times \mathcal{N}$, such that $(i,j) \in \mathcal{L}$, if nodes i,j are connected.Node 0 is assumed to be the substation node with a fixed voltage V_0. Let $B \in \mathbb{R}^{(N+1)\times N}$ be the *incidence matrix* of $\mathcal{G}$ relating the branches in $\mathcal{L}$ to the nodes in $\mathcal{N} \cup \{0\}$, such that the (i,k)-th entry of B is 1 if the i-th node is connected to the k-th branch and, otherwise, 0. Without loss of generality, B can be organized to form an upper-triangular matrix. If V_i and V_j are the voltage phasors at nodes i and j and I_{ij} is the current phasor in

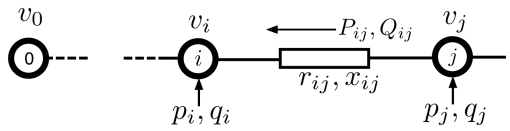

Fig. 2. Nomenclature for a radial distribution network [26].

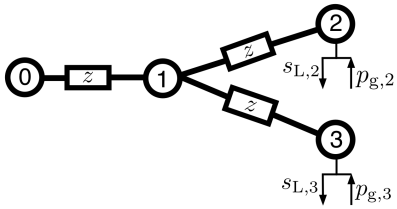

Fig. 3. The 3-node network used as a motivating example.

branch $(i,j)\in\mathcal{L}$, then define $v_i := |V_i|^2$, $v_j := |V_j|^2$ and $l_{ij} := |I_{ij}|^2$. Let P_{ij} (Q_{ij}) be the active (reactive) power flow from node j to i, let p_j (q_j) be the active (reactive) power injections into node j, and let r_{ij} (x_{ij}) be the resistance (reactance) of branch $(i,j)\in\mathcal{L}$, which means that the branch impedance is given by $z_{ij} := r_{ij} + \mathbf{i}x_{ij}$. Then, for a radial network, the relation between node voltages and power flows is given by the *DistFlow* equations $\forall (i,j)\in\mathcal{L}$:

$$v_j = v_i + 2r_{ij}P_{ij} + 2x_{ij}Q_{ij} - |z_{ij}|^2 l_{ij} \tag{1a}$$

$$P_{ij} = p_j + \sum_{h:h\to j} (P_{jh} - r_{jh}l_{jh}) \tag{1b}$$

$$Q_{ij} = q_j + \sum_{h:h\to j} (Q_{jh} - x_{jh}l_{jh}) \tag{1c}$$

$$l_{ij}(P_{ij},Q_{ij},v_j) = \frac{P_{ij}^2 + Q_{ij}^2}{v_j}, \tag{1d}$$

where nodal power injections are $p_j := p_{g,j} - P_{L,j}$ and $q_j := q_{g,j} - Q_{L,j}$ with $p_{g,j}$ ($q_{g,j}$) as the controllable active (reactive) injections and $P_{L,j}$ ($Q_{L,j}$) is the uncontrollable active (reactive) demand. The controllable injections include solar PV and flexible demand.

The goal of this work is to maximize the range of active power DER injections, p_g, from a given feasible operating point with $p_{g,j} = 0, q_{g,j} = 0\ \forall j \in \mathcal{N}$, such that all voltages v_j and currents l_{ij} are within their respective limits (i.e., $v_j \in [\underline{v}_j, \overline{v}_j]\forall j \in \mathcal{N}$ and $l_{ij} \in [\underline{l}_{ij}, \overline{l}_{ij}]\ \forall (i,j) \in \mathcal{L}$). However, finding such a range is challenging due to the non-linear nature of (1d). For clarity, we provide definitions of the following key terms used in the manuscript.

Definition II.1 (AC Admissibility)**.** *A solution of a convex OPF problem is AC admissible, if the solution applied to the original, non-convex AC OPF, which uses* (1)*, is feasible.*

Definition II.2 (Nodal capacity)**.** *Nodal capacity is the range of AC admissible active power injections $\Delta p_{g,j} := [p^-_{g,j}, p^+_{g,j}]\forall j \in \mathcal{N}$ with lower and upper bounds $p^-_{g,j} \le 0$ and $p^+_{g,j} \ge 0$, respectively. That is, for all nodes j, all injections $p_{g,j} \in \Delta p_{g,j}$ are AC admissible.*

In the next section we use a simple 3-node system to motivate the need for analyzing nodal capacity in distribution systems.

B. Motivating example on nodal capacity

Consider the 3-node system shown in Fig. 3. Each branch of the system has an impedance of $z = 0.55 + \mathbf{i}1.33$pu. Node 2 has a load injection $s_{L,2} = -0.02 + \mathbf{i}0.005$pu and node 3 has a load injection $s_{L,3} = -0.015 + \mathbf{i}0.001$pu. Flexible resources $p_{g,2}$ and $p_{g,3}$ are assumed to be located at nodes 2 and 3. Only the active power of resources at nodes 2 and 3 is assumed to be controllable. Based on the sweep of power flow solutions obtained through Matpower [27], by varying $p_{g,2}$ and $p_{g,3}$, Fig. 4 shows the set of the AC OPF for the 3-node system. As can be seen from Fig. 4, the admissible set is non-convex and contains "holes". Hence, it is important when

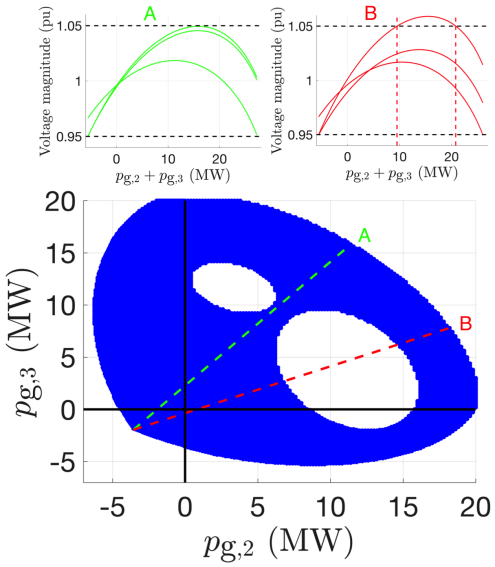

Fig. 4. Analysis of 3-node motivating example. (Bottom) The set of admissible injections is non-convex with trajectories A and B showing admissible (green) and inadmissible (red) dispatch, respectively. (Top) Voltage profiles from sweeping $(p_{g,2}, p_{g,3})$ along admissible trajectory A and inadmissible trajectory B.

dispatching $p_{g,2}$ and $p_{g,3}$, to choose the right trajectory in order to maintain AC admissibility. Figure 4 shows two different dispatch trajectories and the corresponding network voltage profiles obtained along the trajectories. Trajectory A (green) stays within the admissible set and as a result the voltage profile shown in green in the top of Fig. 4, always stays within the constraint limits. If on the other hand, Trajectory B (red) is chosen, then we leave the admissible set which manifests itself in the violation of voltage constraints in the red curve in the top of Fig. 4. Even though trajectory A is AC admissible it requires $p_{g,2}$ and $p_{g,3}$ to be coordinated (i.e., stay on the trajectory) to ensure admissibility, so they cannot be manipulated independently. This means that any changes in either requires a change in the other and, thus, they are not nodal capacities. This is because for nodal capacities, we want the range of injections that can be varied independent of other nodes. This simple example shows the need to develop tools that determines nodal capacities for any radial, balanced network. Towards that objective, the next section develops a convex inner approximation of the non-convex *DistFlow* formulation in (1).

C. Convex Inner Approximation Preliminaries

In this section, we first present a compact matrix representation of the linear components (1a)-(1c). Then, we bound the nonlinear branch current terms in (1d), $l_{ij}(P_{ij}, Q_{ij}, v_j)$, by a convex envelope, which leads to a convex inner approximation of (1).

First, define vectors $P:=[P_{ij}]_{(i,j)\in\mathcal{L}}\in\mathbb{R}^N$, $Q:=[Q_{ij}]_{(i,j)\in\mathcal{L}}\in\mathbb{R}^N$, $V:=[v_i]_{i\in\mathcal{N}}\in\mathbb{R}^N$, $p:=[p_i]_{i\in\mathcal{N}}\in\mathbb{R}^N$, $p_{\mathrm{g}}:=[p_{\mathrm{g},i}]_{i\in\mathcal{N}}\in\mathbb{R}^N$, $P_{\mathrm{L}}:=[P_{\mathrm{L},i}]_{i\in\mathcal{N}}\in\mathbb{R}^N$, $q:=[q_i]_{i\in\mathcal{N}}\in\mathbb{R}^N$, $Q_{\mathrm{L}}:=[Q_{\mathrm{L},i}]_{i\in\mathcal{N}}\in\mathbb{R}^N$, and $l:=[l_{ij}]_{(i,j)\in\mathcal{L}}\in\mathbb{R}^N$ and matrices $R:=\mathrm{diag}\{r_{ij}\}_{(i,j)\in\mathcal{L}}\in\mathbb{R}^{N\times N}$, $X:=\mathrm{diag}\{x_{ij}\}_{(i,j)\in\mathcal{L}}\in\mathbb{R}^{N\times N}$, $Z^2:=\mathrm{diag}\{z_{ij}^2\}_{(i,j)\in\mathcal{L}}\in\mathbb{R}^{N\times N}$, and $A:=[0_N\quad I_N]B-I_N$, where I_N is the $N\times N$ identity matrix and 0_N is a column vector of N rows. Then, directly applying [26], we get the following expression for P, Q and V:

$$V=v_0\mathbf{1}_N+M_{\mathrm{p}}p+M_{\mathrm{q}}q-Hl, \tag{2}$$

$$P=Cp-D_{\mathrm{R}}l,\qquad Q=Cq-D_{\mathrm{X}}l, \tag{3}$$

where matrices $M_{\mathrm{p}}:=2C^TRC$, $M_{\mathrm{q}}:=2C^TXC$, $H:=C^T(2(RD_{\mathrm{R}}+XD_{\mathrm{X}})+Z^2)$ and $C:=(I_N-A)^{-1}$, $D_{\mathrm{R}}:=(I_N-A)^{-1}AR$, and $D_{\mathrm{X}}:=(I_N-A)^{-1}AX$ describe the network topology and impedance parameters. Note that in the authors' previous work in [10], it is shown that the matrix (I_N-A) is non-singular for radial and balanced distribution networks. Furthermore, the convex inner approximation in [25] is valid only for purely inductive, radial, and balanced networks. In this manuscript, the term inductive (capacitive) branch refers to a distribution network branch whose reactance is inductive (capacitive), which means $x_{ij}\geq 0$ ($x_{ij}<0$). In the current manuscript, we extend the convex formulation to any radial and balanced network, including those with mixed inductive and capacitive branches.

Clearly, (2) and (3) represent linear relationships between the nodal power injections, (p,q), the branch power flows, (P,Q), and node voltages V. However, setting $l=0$ and neglecting (1d), as done with the commonly used *LinDist approximation*, can result in overestimating the nodal capacities [10]. Next, we present methods for bounding the nonlinearity $l_{ij}(P_{ij},Q_{ij},v_j)$ from above and below.

Based on the description of voltages in (2) and branch flows in (3), denote l_{lb} and l_{ub} as lower and upper bounds on l. Then, we can define the corresponding upper $(.)^+$ and lower $(.)^-$ bounds of P, Q and V as follows:

$$P^+:=Cp-D_{\mathrm{R}}l_{\mathrm{lb}} \tag{4a}$$

$$P^-:=Cp-D_{\mathrm{R}}l_{\mathrm{ub}} \tag{4b}$$

$$Q^+:=Cq-D_{\mathrm{X}_+}l_{\mathrm{lb}}-D_{\mathrm{X}_-}l_{\mathrm{ub}} \tag{4c}$$

$$Q^-:=Cq-D_{\mathrm{X}_+}l_{\mathrm{ub}}-D_{\mathrm{X}_-}l_{\mathrm{lb}} \tag{4d}$$

$$V^+:=v_0\mathbf{1}_n+M_{\mathrm{p}}p+M_{\mathrm{q}}q-H_+l_{\mathrm{lb}}-H_-l_{\mathrm{ub}} \tag{4e}$$

$$V^-:=v_0\mathbf{1}_n+M_{\mathrm{p}}p+M_{\mathrm{q}}q-H_+l_{\mathrm{ub}}-H_-l_{\mathrm{lb}}, \tag{4f}$$

where D_{X_+} and H_+ include the non-negative elements of D_{X} and H, respectively, and D_{X_-} and H_- are the corresponding negative elements. For example, if the network is purely inductive, then $D_{\mathrm{X}_-}=H_-=0$ and the formulation reduces to the one presented in [25]. These upper and lower bounds in (4) satisfy $P^-\leq P\leq P^+$, $Q^-\leq Q\leq Q^+$ and $V^-\leq V\leq V^+$. Note that the bounds $l_{\mathrm{lb}},l_{\mathrm{ub}}$ in (4) effectively allow us to neglect the nonlinear (1d). Thus, if we can find convex representations of these bounds, the corresponding OPF formulation will be a convex inner approximation. This is described next.

Equation (4) provides a linear formulation for bounding the AC power flow equations in terms of bounds $l_{\mathrm{lb}},l_{\mathrm{ub}}$ and controllable injections. This was first presented in [25], where bounds $l_{\mathrm{lb}},l_{\mathrm{ub}}$ were derived based on a nominal operating point and used to maximize voltage margins with mechanical grid assets (e.g., LTCs and capacitor-banks). Next, we summarize the derivation of these bounds and leverage them to formulate a novel convex inner approximation of the AC OPF to determine the nodal capacities for any radial, balanced network.

Based on any nominal operating point $x_{ij}^0:=\mathrm{col}\{P_{ij}^0,Q_{ij}^0,v_j^0\}\in\mathbb{R}^3$, the second-order approximation for (1d) can be expressed as

$$l_{ij}\approx l_{ij}^0+\mathbf{J}_{ij}^\top\delta_{ij}+\frac{1}{2}\delta_{ij}^\top\mathbf{H}_{\mathrm{e},ij}\delta_{ij}, \tag{5}$$

where $l_{ij}^0:=l_{ij}(x_{ij}^0)$ are squared branch currents and δ_{ij}, Jacobian $\mathbf{J}_{ij}$, and Hessian $\mathbf{H}_{\mathrm{e},ij}$ are defined below:

$$\delta_{ij}:=\begin{bmatrix}P_{ij}-P_{ij}^0\\ Q_{ij}-Q_{ij}^0\\ v_j-v_j^0\end{bmatrix},\ \mathbf{J}_{ij}:=\left.\begin{bmatrix}\frac{\partial l_{ij}}{\partial P_{ij}}\\ \frac{\partial l_{ij}}{\partial Q_{ij}}\\ \frac{\partial l_{ij}}{\partial v_j}\end{bmatrix}\right|_{x_{ij}^0}=\begin{bmatrix}\frac{2P_{ij}^0}{v_j^0}\\ \frac{2Q_{ij}^0}{v_j^0}\\ -\frac{(P_{ij}^0)^2+(Q_{ij}^0)^2}{(v_j^0)^2}\end{bmatrix} \tag{6}$$

$$\mathbf{H}_{\mathrm{e},ij}:=\begin{bmatrix}\frac{2}{v_j^0} & 0 & \frac{-2P_{ij}^0}{(v_j^0)^2}\\ 0 & \frac{2}{v_j^0} & \frac{-2Q_{ij}^0}{(v_j^0)^2}\\ \frac{-2P_{ij}^0}{(v_j^0)^2} & \frac{-2Q_{ij}^0}{(v_j^0)^2} & 2\frac{(P_{ij}^0)^2+(Q_{ij}^0)^2}{(v_j^0)^3}\end{bmatrix}. \tag{7}$$

Thus, the expression in (5) is accurate as we can neglect the third-order term, i.e., the order of accuracy is $\mathcal{O}(||\delta||_\infty^3)$. Furthermore, [25] shows that $\mathbf{H}_{\mathrm{e},ij}$ is positive semi-definite, which, together with (5), means that the lower and upper bounds of l_{ij} for all $(i,j)\in\mathcal{L}$ are given by:

$$l_{ij}=|l_{ij}|\approx|l_{ij}^0+\mathbf{J}_{ij}^\top\delta_{ij}+\frac{1}{2}\delta_{ij}^\top\mathbf{H}_{\mathrm{e},ij}\delta_{ij}| \tag{8}$$

$$\leq|l_{ij}^0|+|\mathbf{J}_{ij}^\top\delta_{ij}|+|\frac{1}{2}\delta_{ij}^\top\mathbf{H}_{\mathrm{e},ij}\delta_{ij}| \tag{9}$$

$$\leq l_{ij}^0+\max\{2|\mathbf{J}_{ij}^\top\delta_{ij}|,|\delta_{ij}^\top\mathbf{H}_{\mathrm{e},ij}\delta_{ij}|\} \tag{10}$$

$$\implies l_{ij}\leq l_{ij}^0+\max\{2|\mathbf{J}_{ij+}^\top\delta_{ij}^+-\mathbf{J}_{ij-}^\top\delta_{ij}^-|,\psi_{ij}\}\leq l_{\mathrm{ub},ij}, \tag{11}$$

$$\text{and } l_{ij}\geq l_{ij}^0+\mathbf{J}_{ij+}^\top\delta_{ij}^--\mathbf{J}_{ij-}^\top\delta_{ij}^+=:l_{\mathrm{lb},ij}, \tag{12}$$

where $\mathbf{J}_{ij+}$ and $\mathbf{J}_{ij-}$ includes the positive and negative elements of $\mathbf{J}_{ij}$, $\delta_{ij}^+:=\delta_{ij}(P_{ij}^+,Q_{ij}^+,v_j^+,x_{ij}^0)$ and $\delta_{ij}^-:=\delta_{ij}(P_{ij}^-,Q_{ij}^-,v_j^-,x_{ij}^0)$, and $\psi_{ij}:=\max\{(\delta_{ij}^{+,-})^\top\mathbf{H}_{\mathrm{e},ij}(\delta_{ij}^{+,-})\}$, which represents the largest of eight possible combinations of $P/Q/v$ terms in δ_{ij} with mixed $+,-$ superscripts. Note that from (12), the lower bound $l_{\mathrm{lb},ij}$ may become negative, however, we know from physics that $l_{ij}\geq 0$, which means the $l_{\mathrm{lb},ij}$ may be overly conservative. Also, from the expression of $\mathbf{J}_{ij}$, it can be seen that if $P_{ij}^0,Q_{ij}^0\approx 0$, then $l_{\mathrm{lb},ij}=l_{ij}^0\approx 0$ and so the lower bound is fixed for this operating point. This results in an overly conservative estimate of the lower bound, which can result in conservative nodal hosting capacity results. To alleviate this shortcoming, Algorithm 1 in Section III-B presents an iterative approach that improves the nodal capacity. Thus, from (4), (11), and (12) we have a convex inner approximation of (1) that can be used to determine the nodal capacities. Furthermore, since the Jacobian and Hessian are calculated separately for each branch in the network, the size of the matrices does not grow with the size of the system. This enables the extension of this approach to large scale systems.

D. Optimizing DER nodal capacity

The bounds from (12) and (11) allow us to omit (1d) entirely and replace the original variables P, Q, and V with their corresponding

upper and lower bounds $(.)^+$ and $(.)^-$ in (4). Since $(.)^+$ and $(.)^-$ are outer approximations, using them in an OPF formulation results in a feasible set that is contained in the original, non-convex AC OPF, which means that (P1) below represents a convex inner approximation and can be used to determine nodal hosting capacities:

$$\text{(P1)} \quad p_g^+(p_g^-) = \arg\min_{p_{g,i}, q_{g,i}} \sum_{i=1}^{N} f_i(p_{g,i}) \tag{13}$$

$$\text{s.t.} \quad \text{(4a)}-\text{(4f)},(11),(12) \tag{14}$$

$$p = p_g - P_L \quad q = q_g - Q_L, \tag{15}$$

$$\underline{V} \le V^-(p,q) \quad V^+(p,q) \le \overline{V} \tag{16}$$

$$l_{ub} \le \bar{l} \quad \underline{q_g} \le q_g \le \overline{q_g} \tag{17}$$

where (16) ensure that any feasible dispatch p_g from (P1) satisfies the nodal voltages in the original AC OPF based on (1). Also, the current limit constraint in (17) ensures that the upper limit of the branch current (l_{ub}) is within the given thermal line current limits. To determine the nodal capacity , we must solve (P1) once for the lower range, p_g^-, and once for the upper range, p_g^+. Thus, the objective function components, $f_i(p_{g,i})$, must be designed to engender $p_{g,i}^-$ and $p_{g,i}^+$. For example, to compute $p_{g,i}^-$, we can choose $f_i(p_{g,i}) := \alpha_i p_{g,i}$ and, for $p_{g,i}^+$, we can designate $f_i(p_{g,i}) := -\alpha_i p_{g,i}$, where α_i is the relative priority of nodal capacity at node i. Clearly, the choice of objective function determines how flexibility is allocated over the network nodes, e.g., choosing objective function such as $\pm\alpha_i \log(p_{g,i})$ could result in a different allocation of nodal capacity over the nodes as compared with $\pm\alpha_i p_{g,i}$. The design of the objective function represents an interesting future extension into energy policy and incentive mechanism and rate design [28].

While (P1) ensures AC admissibility at the nodal capacity values, it is natural to consider what happens when the nodal flexibility is below the rated capacity. That is, are all injections within the hosting capacity range guaranteed to be admissible across all the nodes? The next section answers this question by providing analytical guarantees of admissibility for the nodal hosting capacity, Δp_g, and then presents an iterative algorithm to successively improve Δp_g.

III. Analysis of Convex Inner Approximation

Next, we analyze (P1) and prove that $p_g \in \Delta p_g$ is AC admissible.

A. Admissibility guarantees

To prove admissibility claims below, we only present nodal voltages (as the case of branch flows is similar). Theorem III.1 shows that the range Δp_g obtained through (P1) results in an AC admissible load flow solution.

Theorem III.1. *Under conditions C1) $\frac{\partial V^+}{\partial p_{g,i}} \ge 0$, C2) $\frac{\partial V^-}{\partial p_{g,i}} \ge 0$, $\forall i \in \mathcal{N}$, if Δp_g is the DER nodal capacity obtained via (P1), then $\forall p_g \in \Delta p_g$ and $p(p_g) = p_g - P_L$, we have*

$$\underline{V} \le V^-(p) \le V(p) \le V^+(p) \le \overline{V},$$

where $V(p)$ represents the actual nodal voltages from (1).

Proof. Consider two cases: Case 1: $0 \le p_g \le p_g^+$; and Case 2: $0 \ge p_g \ge p_g^-$.
Proof of Case 1: Using (4e) at p_g^+ yields:

$$V^+(p^+) = v_0 \mathbf{1}_n + M_p p^+ + M_q q^+ - H_+ l_{lb} - H_- l_{ub} \le \overline{V} \tag{18}$$

where $p^+ = p_g^+ - P_L$ and $q^+ = q_g^+ - Q_L$. Now, consider any $p_g \in \Delta p_g$ such that $0 \le p_g \le p_g^+$ and using C1, then

$$V^+(p) = v_0 \mathbf{1}_n + M_p p + M_q q^+ - H_+ l_{lb}(p) - H_- l_{ub}(p) \le \overline{V} \tag{19}$$

where $p = p_g - P_L$. The actual voltage according to (2) at p is

$$V(p) = v_0 \mathbf{1}_n + M_p p + M_q q^+ - H_+ l(p) - H_- l(p) \tag{20}$$

Then, subtracting (19) from (20) gives:

$$V^+(p) - V(p) = H_+(l(p) - l_{lb}(p)) + H_-(l(p) - l_{ub}(p)) \tag{21}$$

Using (12) and (11) we get, $l_{lb}(p) \le l(p) \le l_{ub}(p)$ and that $V^+(p) - V(p) \ge 0 \implies V(p) \le V^+(p) \le \overline{V}$.
Proof of Case 2: Using (4f) at p_g^- yields:

$$V^-(p^-) = v_0 \mathbf{1}_n + M_p p^- + M_q q^- - H_+ l_{ub} - H_- l_{lb} \ge \underline{V} \tag{22}$$

where $p^- = p_g^- - P_L$ and $q^- = q_g^- - Q_L$. Now, consider any $p_g \in \Delta p_g$ such that $0 \ge p_g \ge p_g^-$ and C2, then

$$V^-(p) = v_0 \mathbf{1}_n + M_p p + M_q q^- - H_+ l_{ub}(p) - H_- l_{lb}(p) \ge \underline{V} \tag{23}$$

where $p = p_g - P_L$. The actual voltage according to (2) at p is

$$V(p) = v_0 \mathbf{1}_n + M_p p + M_q q^- - H_+ l(p) - H_- l(p) \tag{24}$$

Then, subtracting (23) from (24) gives:

$$V^-(p) - V(p) = H_+(l(p) - l_{ub}(p)) + H_-(l(p) - l_{lb}(p)) \tag{25}$$

Using (12) and (11) we get, $l_{lb}(p) \le l(p) \le l_{ub}(p)$, and that $V^-(p) - V(p) \le 0 \implies V(p) \ge V^-(p) \ge \underline{V}$. Case 1 and Case 2 complete the proof. □

Conditions C1 and C2 may not always hold. This can be seen from (4e) and (4f), as V^+ and V^- depend on the upper bound l_{ub} of the loss term l. This upper bound in turn is based on the expression in (11) and can either increase or decrease with p. This is further illustrated in Fig. 4, which shows that the voltage magnitude decreases with increase in power injection after a certain threshold is crossed. Furthermore, condition C1 and C2 only guarantee satisfaction of network constraints over the nodal capacity and do not provide guarantees for existence of power flow solutions. Guarantees on existence of solutions will be provided in Section III.D. Theorem III.1 significantly improves over the result provided in [25], since it guarantees that the full range, Δp_g, is admissible rather than just the solutions, p_g^+ and p_g^-. Importantly, this is *exactly* why Δp_g can be used to represents the nodal hosting capacity. As with any convex inner approximation, the results can be conservative. Thus, in the next section, a new iterative algorithm is presented that successively increases the nodal capacity.

B. Iterative Algorithm for nodal capacity improvement

The lower and upper bounds obtained in section II-C can be conservative initially depending upon the nominal operating point, x^0. Without Algorithm 1, when we solve (P1) to determine p_g^+ and p_g^-, the nodal capacities can be significantly underestimated. This is because the operating point x^0 in certain situations could be such that, $P_{ij}^0 = Q_{ij}^0 \approx 0$, which means that the Jacobian would be close to zero and the first-order estimate of $l_{lb,ij}$ would be close to $l_{ij}^0 \approx 0$ per (12). Without Algorithm 1, after solving (P1), the result could be a very conservative inner approximation, which would lead to an

under-estimate of the hosting capacity. Algorithm 1 overcomes this by successively enhancing the feasible set by updating the operating point and the Jacobian (and the Hessian) with the optimized decision variables, sometimes called the convex-concave procedure [29]. Algorithm 1 outlines the steps involved in the proposed scheme.

Algorithm 1: Successive enhancement of DER nodal capacity Δp_{g} (unity power factor case)

Result: Admissible range $\Delta p_{\mathrm{g}} = [p_{\mathrm{g}}^{-}, p_{\mathrm{g}}^{+}]$
1 **Input:** $P_L, Q_L \in \mathbb{R}^N$, convex $f_i(p_{\mathrm{g},i}) \forall i \in \mathcal{N}$, and $\epsilon > 0$
2 Run Load flow w/ $P_L, Q_L, p_{\mathrm{g}}(0) = 0 \Rightarrow \mathbf{J}(0), \mathbf{H}_{\mathrm{e}}(0)$
3 **for** $m = 1:2$ **do**
4 **if** $m = 1$ **then**
5 $p_{\mathrm{g},i} \to p_{\mathrm{g},i}^{+}$, Cond$(i) \to$ Check $\frac{\partial V^{+}}{\partial p_{\mathrm{g},i}} \geq 0 \quad \forall i \in \mathcal{N}$
6 **else**
7 $p_{\mathrm{g},i} \to p_{\mathrm{g},i}^{-}$, Cond$(i) \to$ Check $\frac{\partial V^{-}}{\partial p_{\mathrm{g},i}} \geq 0 \quad \forall i \in \mathcal{N}$
8 **end**
9 Initialize $k = 1$, $error(0) = \infty$
10 **while** $\exists i$, *s.t. Cond(i) holds* $\wedge$ $error(k-1) > \epsilon$ **do**
11 **for** $i = 1:N$ **do**
12 **if** *Cond(i) does not hold* **then**
13 Set $p_{\mathrm{g},i}(k) = 0$
14 **end**
15 **end**
16 Solve (P1) $\Rightarrow p_{\mathrm{g},i}(k), f_i(p_{\mathrm{g},i}(k)), \forall i \in \mathcal{N}$
17 Run load flow w/ $P_L - p_{\mathrm{g}}(k), Q_L \Rightarrow \mathbf{J}(k), \mathbf{H}_{\mathrm{e}}(k)$
18 Update Cond(i) $\forall i \in \mathcal{N}$
19 Update error:
20 $error(k) = \max_{i \in \mathcal{N}} |f_i(p_{\mathrm{g},i}(k)) - f_i(p_{\mathrm{g},i}(k-1))|$
21 $k \to k+1$
22 **end**
23 **end**

Next, we apply Algorithm 1 to the motivating example from Fig. 3 to present how the nodal capacity is improved. Note that reactive power net injections, $q_{\mathrm{g},i}$, are decision variables in (P1), however, in the proceeding analysis and simulations, we set $q_{\mathrm{g},i} = 0$.[1] Later in Section IV, we analyze the role of reactive power strategies in enabling greater DER nodal capacities. For the sake of simplicity, we neglect the branch limit constraint (17) in (P1) and assume an oversized substation transformer, which is a common practice in the US. The focus is on voltage because that is often the primary concern of utilities in the US [30]. However, the formulation in (P1) and the analysis therein hold for branch limit constraints as well. Future work will analyze and provide simulation results on this extension.

If Algorithm 1 is applied to determine p_{g}^{+} and p_{g}^{-} without considering C1 and C2 (i.e, omit lines 12-14 in Algorithm 1), then the admissible set for $p_{\mathrm{g},2}$ and $p_{\mathrm{g},3}$ is shown by the blue region in Fig. 5. When the conditions C1 and C2 are considered in Algorithm 1, then the green region in Fig. 5 is the admissible set. As can be seen from the figure, the green region is a convex set that is contained in the blue set as expected from being a convex inner approximation. The successive iterative solutions obtained through Algorithm 1 are also

[1]For this manuscript, any mechanical devices such as tap-changers, capacitor banks and switches are assumed to be fixed at their nominal values and are not part of the optimization problem.

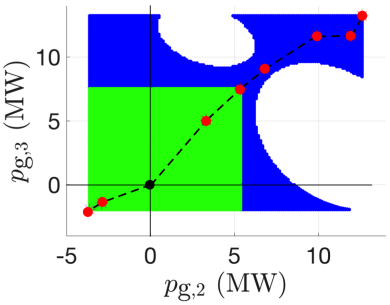

Fig. 5. The set of admissible injections for the 3-node network is non-convex (blue). Algorithm 1 can find maximal admissible injections via iterations (red dots), but monotonicity conditions $C1$ and $C2$ in Theorem III.1 define the convex inner approximation (green), which gives nodal capacity Δp_{g}.

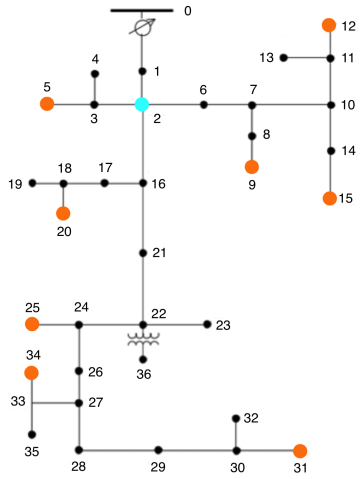

Fig. 6. Single-phase version of the IEEE-37 node distribution network from [31].

marked in Fig. 5. It is clear from the non-convex nature of the blue set that operating in that region would require coordination between different nodes in order to ensure AC admissibility (i.e., to stay on the piece-wise linear trajectory provided by the iterates with the black dotted line in Fig. 5). On the other hand, since the green set is a hypercube, no coordination between nodes is necessary in order to guarantee AC admissibility. Due to these reasons, further analysis in this work will consider this hypercube AC admissible region only. The analysis shown here provides a mechanism to update the operating point to achieve larger DER nodal capacity.

Next, we present Case Study 1, which employs Algorithm 1 to determine the solar PV hosting capacity for a distribution network.

Case study 1: Algorithm 1 is applied to the IEEE-37 node distribution feeder shown in Fig. 6 for three different scenarios to determine $p_{\mathrm{g},i}^{+}$. The orange and cyan dots in Fig. 6 represent the location of the solar PV in the network. In this context, $p_{\mathrm{g},i}^{+}$ can effectively be considered the solar PV hosting capacity. The three different scenarios are specified in Table I. In scenarios A (linear objective) and B (logarithmic objective), the solar PV units may be installed at the leaf nodes with the largest demand, whereas in scenario C (linear objective), solar PV is only allowed at node 702 (e.g., utility-scale solar PV array). The optimization problem (P1) is solved with Gurobi 9.1 in Julia 1.1 in less than 1 sec and the solution

TABLE I
PV HOSTING CAPACITY SCENARIOS

Scenario	Nodes with PVs	Objective function
A	{5,9,12,15,20,25,31,34}	$f_i(p_{g,i}) = -p_{g,i}$
B	{5,9,12,15,20,25,31,34}	$f_i(p_{g,i}) = -\log(p_{g,i})$
C	{2}	$f_i(p_{g,i}) = -p_{g,i}$

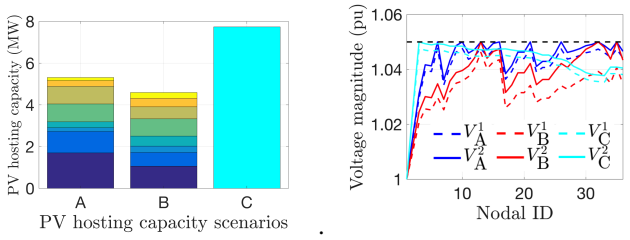

(a) (b)

Fig. 7. Case study 1 on IEEE-37 node network for the three PV scenarios. (a) Shows the feeder's solar PV hosting capacity with Algorithm 1. (b) illustrates admissibility of PV hosting capacity via voltage profiles, where V_A^1, V_B^1, V_C^1 results from first iteration and V_A^2, V_B^2, V_C^2 are from final iteration of Algorithm 1.

is validated with Matpower [27] on a standard MacBook Pro laptop with 2.2GHz CPU and 16GB RAM. The comparison of the resulting solar PV hosting capacity from each scenario using Algorithm 1 is shown in Fig. 7a, with the stacked bars showing the hosting capacity at the different nodes with DERs in the system. For each of the scenarios A, B, and C, the stacks in the bar charts represent the different nodes with PVs as shown in Table I. It can be seen that having a single centralized solar unit allows greater total solar PV capacity as compared to the distributed cases. The reason for this is that Scenario C has fewer network limit constraints to consider than the distributed case. This can be seen from Fig. 7b which shows voltages obtained for the three scenarios at the first iteration PV hosting capacity and after repeated iterations through Algorithm 1. As can be seen from the figure, voltages are at their upper limit at multiple nodes for scenarios A and B, but only at the head-node (node 2) for scenario C. As a result, the distributed case (case A and B) has more active constraints and hence more conservative solution as compared to the case with a single central PV (case C). Furthermore, scenario B favors a more equitable allocation (log objective) that results in smaller net solar PV capacity ($\sum_i p_{g,i}$), leading to reduced overall performance as compared to scenario A. The results show the admissibility of the PV hosting capacity solution both by using (P1) once or repeatedly through Algorithm 1. The results in Case Study 1 show the nodal hosting capacity when different weights are allocated to different nodes. This approach can be relevant to align available hosting capacity with incentives that prioritize certain load pockets or to ensure an equitable distribution of dispatchable DERs.

C. Quantifying conservativeness

In this section, we present simulation-based analysis to quantify the conservativeness of the convex inner approximation. We show how iterative Algorithm 1 enlarges the CIA. The results are shown in Table II for the IEEE-13 node and IEEE-37 node systems, respectively. The table shows how the nodal capacity is increased for the three scenarios (A, B, and C) between the iterations in Algorithm 1. The results show that Algorithm 1 reduces the conservativeness of the CIA method and improve hosting capacity.

TABLE II
FEEDER SOLAR PV HOSTING CAPACITY INCREASE WITH ITERATIONS IN ALGORITHM 1 FOR (A) IEEE-13 NODE SYSTEM AND (B) IEEE-37 NODE SYSTEM.

(a)

Iteration	A	B	C
Iter 1 (MW)	6.6	6.3	8.8
Iter 2 (MW)	9.1	8.6	12.1

(b)

Iteration	A	B	C
Iter 1 (MW)	5.1	4.4	7.4
Iter 2 (MW)	5.3	4.6	7.7

Furthermore, to compare the convex inner approximation method with other techniques in literature, such as using a convex relaxation method or solving a non-linear program (NLP) using Interior point solvers, we present comparisons in Table III. The second order cone program (SOCP) uses a conic relaxation of the power flow equations to obtain a convex formulation, where as the NLP solves the original non-convex problem using IPOPT. The SOCP relaxation provides an upper bound on the nodal capacity, but can lead to solutions that are not physically realizable, i.e., violate system constraints. On the other hand, NLP may lead to optimal solutions that are local instead of global. Furthermore, the resulting NLP solution can only guarantee the points (p_g^-, p_g^+) are admissible but cannot guarantee that the entire range $[p_g^-, p_g^+]$ is admissible. The proposed CIA approach, on the other hand, guarantees not only that voltages and currents are within their limits over the entire range, but also that the nodal injections can be manipulated independently over their ranges. These results provide a measure of the conservativeness of the convex inner approximation. The results in Table III show the lower and upper bound of the hosting capacity for three distribution systems (13 node, 37 node and 123 node). The results show that the CIA solution is similar to the NLP solution. Thus, the hosting capacity is not overly conservative. The SOCP results, even though much larger, are not physically realizable, i.e., they violate network constraints. This comparison shows the effectiveness of the proposed approach in obtaining nodal capacity limits while guaranteeing satisfaction of network constraints.

The CIA optimization is solved with Gurobi 9.1 in Julia 1.1 with the IEEE-123 node system solving in less than 10 sec on a standard MacBook Pro laptop with 2.2GHz CPU and 16GB RAM

TABLE III
COMPARING HOSTING CAPACITY RESULTS USING CONVEX INNER APPROXIMATION WITH CONVEX RELAXATION (CR) AND NON-CONVEX (NLP) FORMULATIONS

System	CIA (MW)	NLP (MW)	CR (MW)
13-node	[-1.5, 9.1]	[-1.5, 9.7]	[-1.5, 12]
37-node	[-2.7, 5.3]	[-2.7, 5.3]	[-2.7, 16]
123-node	[-4.5, 13.9]	[-4.5, 14]	[-4.5, 24]

Remark (Adapting analysis to distribution planning)**.** *It is important to note that the nodal capacity in this network can incorporate both generation ($p_g^+ > 0$) and flexible demand ($p_g^- < 0$), but that Δp is with respect to a particular operating point, (P_L, Q_L). This is different from conventional PV hosting capacity studies that consider a representative annual, hourly demand profile [30]. In future work, we will adapt (P1) and Algorithm 1 for multi-hour planning problems and incorporate battery storage and flexible*

demand to determine the "dynamic hosting capacity" of a feeder from quasi-static timeseries (QSTS) demand profiles.

D. Existence and uniqueness of power flow solution

If a solution to the power flow equations in (1) exists, the convex inner approximation (CIA) approach presented herein guarantees satisfaction of network constraints over the range of nodal capacities, $p_g \in [p_g^-, p_g^+]$. However, the CIA approach alone does not guarantee existence of a power flow solution. Early work on the existence of power flow solutions in radial distribution networks showed that a unique solution exists for a wide range of practical parameter values [32]. However, there are power injections for which a solution may not exist, but such cases often occur under impractical operating conditions [33]. Nonetheless, ensuring existence of solutions for the entire range of nodal capacities is valuable. Recent works in literature, e.g., [34], have provided sufficient conditions for the existence and uniqueness of a solution to (1). This has since been extended to multi-phase distribution networks [35]. The existence of power flow solutions is also closely related to the voltage collapse problem and has been studied in [36]. In this section, we utilize sufficient conditions from [34], to provide guarantees for both the satisfaction of network constraints and the existence of a solution over the range of nodal capacities. In this regard, we augment Algorithm 1 with two additional conditions that are adapted from [34]. The first condition ensures a solution exists at the current operating point of Algorithm 1, i.e., $x_{ij}^0 = \text{col}\{P_{ij}^0, Q_{ij}^0, v_j^0\} \quad \forall (i,j) \in \mathcal{L}$. This condition is given by:

$$\zeta(\hat{s}) < u_{\min}^2 \tag{26}$$

where $\zeta(\hat{s})$ and $u_{\min}$ are defined as:

$$\zeta(s) := ||W^{-1} Y_{\text{LL}}^{-1} \overline{W}^{-1} diag(\overline{s})||_\infty \tag{27}$$

$$u_{\min} := \min_j |V_j^0 / w_j| \tag{28}$$

with $W := diag(w)$, $w := -Y_{\text{LL}}^{-1} Y_{\text{L0}}$, $s = p + \mathbf{i}q$ is the complex nodal power injection, $\hat{s} = -P_{\text{L}} - \mathbf{i}Q_{\text{L}}$, and Y is the admittance matrix such that

$$Y = \begin{bmatrix} Y_{00} & Y_{0\text{L}} \\ Y_{\text{L0}} & Y_{\text{LL}} \end{bmatrix}.$$

Condition (26) can be readily checked in Algorithm 1 at the operating point before each iteration.

The second condition is incorporated into (P1) as follows. Define $s = \hat{s} + s_g$, where $s_g = p_g + \mathbf{i}q_g$. We can then determine sufficient conditions for existence of a solution over the range of nodal capacities $p_g^- \le p_g \le p_g^+$. Thus, the following constraint is added to (P1).

$$\Delta := \left(u_{\min} - \frac{\zeta(\hat{s})}{u_{\min}} \right)^2 - 4\zeta(s_g) > 0. \tag{29}$$

Defining $\chi := (u_{\min} - \frac{\zeta(\hat{s})}{u_{\min}})^2/4$ and $A^{\text{w}} := W^{-1} Y_{\text{LL}}^{-1} \overline{W}^{-1}$, the condition in (29) then becomes $||A^{\text{w}} diag(s_{\text{g}})||_\infty < \chi$, which from the definition of matrix norm can be expressed as

$$\max_{i=1,\ldots,N} \sum_{j=1}^{N} |A_{ij}^{\text{w}} \overline{s}_{\text{g},j}| < \chi. \tag{30}$$

The constraint in (30) can also be represented by N constraints of the form $\sum_{j=1}^{N} |A_{ij}^{\text{w}} \overline{s}_{\text{g},j}| < \chi \quad \forall i = 1,\ldots,N$. By defining $A_{ij}^{\text{w}} = a_{ij}^{\text{w}} + \mathbf{i} b_{ij}$ and using and expanding the complex product, we get the following equivalent convex formulation of (29) that is composed of N linear inequalities and N second-order cone (SOC) constraints:

$$\begin{aligned} &\sum_{j=1}^{N} t_{ij} < \chi \quad \forall i = 1,\ldots,N \\ &\left|\left| \begin{bmatrix} a_{ij}^{\text{w}} & b_{ij}^{\text{w}} \\ b_{ij}^{\text{w}} & -a_{ij}^{\text{w}} \end{bmatrix} \begin{bmatrix} p_{\text{g},j} \\ q_{\text{g},j} \end{bmatrix} \right|\right|_2 \le t_{ij} \quad \forall j = 1,\ldots,N. \end{aligned} \tag{C3}$$

The reformulation in (C3) can now be readily included in (P1) when computing the nodal capacities. To investigate the conservativeness of the CIA method with (C3), Table IV compares the hosting capacity with and without (C3) on the IEEE-13 node, 37-node and 123-node networks. The results indicate that including (C3) leads to meaningful and practical solutions similar to the results in Section III-C.

TABLE IV
COMPARING PROPOSED CONVEX INNER APPROXIMATION WITH AND WITHOUT EXISTENCE CONDITION (C3)

Type	13-node	37-node	123-node
Without C3 (MW)	[-1.5, 9.1]	[-2.7, 5.3]	[-4.5, 13.9]
With C3 (MW)	[-1.5, 8.8]	[-2.7, 5.3]	[-4.5, 13.8]

The analysis and simulation results presented in case study 1 and this section have used $q_{\text{g}} = 0$, e.g., unity power factor solar PV arrays. However, the role of reactive power management in optimizing DER nodal capacities is important and the focus of the next section.

IV. Role of Reactive Power

Reactive power, q_{g}, can be utilized to increase the nodal capacity, $[p_{\text{g}}^-, p_{\text{g}}^+]$. Different reactive power control schemes are analyzed in this section. Specifically, we will compare between DERs that are operated at unity power factor, fixed power factor, and those with reactive power control capability, where the power factor is allowed to vary according to advanced inverter capabilities, such as IEEE Standard 1547 [37]. The different reactive power schemes along with the relevant relations between q_{g} and p_{g} are provided in Table V. For each particular scheme, the corresponding constraints are added to (P1) when determining the nodal capacity.

Fig. 8a compares the feeder's solar PV hosting capacities, $\sum_i p_{\text{g},i}^+$, resulting from the different reactive power schemes applied to Scenario A of Case Study 1. The stacked bar chart in Fig. 8a also shows the hosting capacity at the different nodes with DERs in this system. Scheme UPF represents the hosting capacity with unity power factor, which matches the result from Scenario A in Fig. 7a and serves as the base-case for comparison. Scheme LAG employs a lagging power factor of 0.95 ($\gamma_i = -0.33$), while LEAD uses a leading power factor of 0.95 ($\gamma_i = +0.33$). Scheme QVP employs a common volt-VAr policy with $\beta_i^0 = 0$ and $\beta_i^1 = -0.073$, while QCON represents advanced inverter capability with quadratic constraints and $\bar{S}_{\text{g},i} = 2$MVA and a minimum power factor of 0.95. The results show that for scheme LEAD, the hosting capacity is reduced while schemes LAG, QCON and QVP increase hosting capacity. In LEAD, this is due to reactive power injections increasing with active power injections resulting in larger v and, hence, reduces

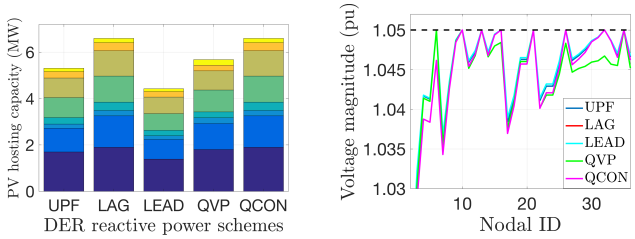

(a) (b)

Fig. 8. Reactive power schemes for case Study 1 (Scenario A) on the IEEE-37 node network for five different reactive power schemes: (a) Solar PV hosting capacity for each reactive power scheme after employing Algorithm 1 (b) Illustrating admissibility with voltage profiles for the final iterate from Algorithm 1.

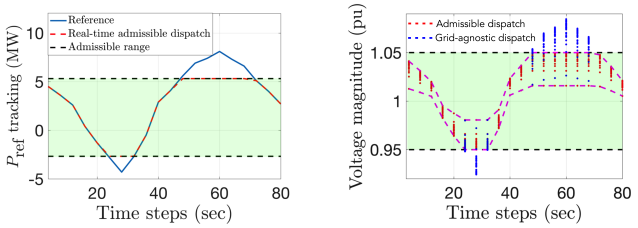

(a) (b)

Fig. 9. Case study 2: (a) tracking performance of the realtime disaggregation policy shown in (31) for IEEE-37 node system (b) Voltage profile of the IEEE-37 node network over the time steps showing the admissibility of the solution when following the disaggregation policy (red) and voltage violations when following the greedy approach (blue). The greedy approach results in a maximum voltage violation of 0.03 pu at time-step 60.

p_{g}^{+}. The opposite occurs in the other schemes. Interestingly, QCON achieves the same nodal capacity as LAG at minimum power factor (0.95). This shows that reactive power scheme in QCON chooses the minimum power factor injection in order to maximize nodal capacity. The voltage profiles at the hosting capacities for the different schemes are compared in Fig. 8b and are clearly AC admissible. The results in Fig. 8 show the increased hosting capacity when reactive power control is utilized. As many DERs have certain reactive power capabilities, including solar PV inverters, it is valuable to study the impact of advanced inverter functionality on the nodal hosting capacities. This is in line with the development of reactive power requirements and standards of these devices [37].

TABLE V
DER REACTIVE POWER SCHEMES

Scheme	Description	Constraint ($g_i(p_{\text{g},i},q_{\text{g},i},v_i)$)
UPF	Unity power factor	$q_{\text{g},i}=0$
LAG	Lagging power factor	$q_{\text{g},i}=-\gamma_i p_{\text{g},i}$
LEAD	Leading power factor	$q_{\text{g},i}=\gamma_i p_{\text{g},i}$
QVP	Volt-VAr policy	$q_{\text{g},i}=\beta_i^0+\beta_i^1 v_i$
QCON	Quadratic constraint	$p_{\text{g},i}^2+q_{\text{g},i}^2\le \bar{S}_{\text{g},i}^2$

The next section employs the nodal capacities, $\Delta p_{\text{g},i}$, to develop a simple, open-loop, decentralized DER control policy for the realtime, grid-aware disaggregation of a (net) demand reference signal. This turns the whole feeder into a responsive grid resource with *a-priori* AC admissibility guarantees that can provide fast grid services in wholesale markets.

V. Realtime Grid-Aware Disaggregation

Dispatching a set of networked DERs in response to a fast, time-varying wholesale market signal while guaranteeing admissible operations is challenging. However, it is necessary to solve this problem before aggregators can safely coordinate millions of behind-the-meter DERs without jeopardizing reliability of the grid. Thus, after computing the available nodal capacity (offline), as shown in Fig. 1, this section proposes a simple, grid-aware controller to allocate the required flexibility among the available resources in the network (i.e., disaggregate the signal) in realtime. The advantage of such a mechanism is that it simplifies the interface between the distribution system operator (DSO) and the individual aggregators. The DSO has the responsibility of determining DER nodal capacities for each aggregator, whereas the aggregator is only required to operate within the provided nodal capacities. This is realistic as the DSO has access to the network data while the aggregators do not. Hence, this method acts as a bridge between the DSO and aggregators, taking advantage of each of their strengths, in order to enable reliable, real-time dispatch of DERs.

The necessary parameters to execute the realtime, grid-aware disaggregation are $p_{\text{g},i}^{+}$ and $p_{\text{g},i}^{-}$ and can be updated every 15-60 minutes by the grid operator running Algorithm 1, which is the timescale of the baseline of the aggregate uncontrollable net-demand.

The realtime disaggregation can then be solved by a DER aggregator to provide fast grid service without the need to include *any* information about the underlying grid parameters. That is, the nodal capacities embed the AC OPF constraints to simplify the aggregator's dispatch. The disaggregation process is determined by the following open-loop policy:

$$p_{\text{g},i}[k]=\begin{cases}\min\{\frac{p_{\text{g},i}^{+}}{\sum_i p_{\text{g},i}^{+}}P_{\text{ref}}[k],p_{\text{g},i}^{+}\} & P_{\text{ref}}[k]\ge 0\\ \max\{\frac{p_{\text{g},i}^{-}}{\sum_i p_{\text{g},i}^{-}}P_{\text{ref}}[k],p_{\text{g},i}^{-}\} & P_{\text{ref}}[k]<0\end{cases} \tag{31}$$

The next case study shows the effectiveness of the proposed disaggregation process in having DERs collectively respond to grid service signals while guaranteeing AC admissibility. Future work will consider the role of feedback and disturbances.

Case study 2: The effectiveness of the offline Algorithm 1 and the online disaggregation in (31) is illustrated in a second case study with the IEEE-37 node system where we use the nodal capacities defined by Scenario A. The case study shows that the feeder is being managed within its limits at all times despite providing a large range of flexibility from the responsive DERs. Fig. 9a shows a reference grid service signal and the aggregate response from dispatching the DERs. It can be seen that the reference market signal is tracked well when the reference is within the admissible range and the grid-aware dispatch is AC-admissible as shown in Fig. 9b. In a practical setting, the DER aggregator should only offer what can be delivered, but the case study is meant to illustrate how the realtime dispatch is grid-aware and how the nodal capacities can be used to easily define the admissible range. Clearly, if the aggregator was not grid aware and just coordinated DERs to ensure perfect tracking, then such a "greedy" version of the realtime DER control leads to violations in network voltages, as seen by the blue dots in Fig. 9b. Thus, the proposed open-loop control scheme is grid-aware and scalable across a network of DERs by just broadcasting a single scalar grid service reference.

VI. Conclusions and Future work

This manuscript presents a convex inner approximation of the AC OPF problem. Leveraging convex lower and upper bounds on the nonlinear branch flow terms in the AC formulation, the inner approximation ensures an AC admissible optimal solution. A novel algorithm is presented to successively improve the nodal capacity values of a feeder. Reactive power control schemes are then presented and volt-VAr and smart inverter schemes are shown to further improve the nodal capacity. Finally, a realtime disaggregation scheme is presented for dispatching flexible demand in realtime across the network, while respecting the grid constraints and providing fast grid services.

Future work will extend this work to multi-phase feeder models and meshed networks to account for more realistic distribution feeders. Optimizing legacy and other front-of-meter grid asset schedules to increase or maintain the nodal hosting capacities is also of interest. Finally, employing feedback from salient grid measurements to provide robust admissibility guarantees in realtime under changes to expected demand/solar PV is another important area to investigate.

References

[1] J. Driesen and R. Belmans, "Distributed generation: Challenges and possible solutions," in *Power Engineering Society General Meeting, 2006. IEEE*. IEEE, 2006, pp. 8–pp.

[2] H. Hao, B. M. Sanandaji, K. Poolla, and T. L. Vincent, "Aggregate flexibility of thermostatically controlled loads," *IEEE Transactions on Power Systems*, vol. 30, no. 1, pp. 189–198, 2014.

[3] S. H. Tindemans, V. Trovato, and G. Strbac, "Decentralized control of thermostatic loads for flexible demand response," *IEEE Transactions on Control Systems Technology*, vol. 23, no. 5, pp. 1685–1700, 2015.

[4] F. L. Müller, J. Szabó, O. Sundström, and J. Lygeros, "Aggregation and disaggregation of energetic flexibility from distributed energy resources," *IEEE Transactions on Smart Grid*, vol. 10, no. 2, pp. 1205–1214, 2017.

[5] L. Kristov, P. De Martini, and J. D. Taft, "A tale of two visions: Designing a decentralized transactive electric system," *IEEE Power and Energy Magazine*, vol. 14, no. 3, pp. 63–69, 2016.

[6] J. Carpentier, "Contribution to the economic dispatch problem," *Bulletin de la Societe Francoise des Electriciens*, vol. 3, no. 8, pp. 431–447, 1962.

[7] D. K. Molzahn, "Computing the feasible spaces of optimal power flow problems," *IEEE Transactions on Power Systems*, vol. 32, no. 6, pp. 4752–4763, 2017.

[8] D. K. Molzahn and I. A. Hiskens, "A Survey of Relaxations and Approximations of the Power Flow Equations," *Foundations and Trends in Electric Energy Systems*, vol. 4, no. 1-2, pp. 1–221, 2 2019.

[9] M. Baran and F. F. Wu, "Optimal sizing of capacitors placed on a radial distribution system," *IEEE Transactions on power Delivery*, vol. 4, no. 1, pp. 735–743, 1989.

[10] N. Nazir and M. Almassalkhi, "Convex inner approximation of the feeder hosting capacity limits on dispatchable demand," *In: IEEE Conference on Decision and Control (to appear). Nice, France*, 2019.

[11] K. Dvijotham and D. K. Molzahn, "Error bounds on the DC power flow approximation: A convex relaxation approach," in *Decision and Control (CDC), 2016 IEEE 55th Conference on*, 2016, pp. 2411–2418.

[12] S. Bolognani and F. Dörfler, "Fast power system analysis via implicit linearization of the power flow manifold," in *2015 53rd Annual Allerton Conference on Communication, Control, and Computing (Allerton)*. IEEE, 2015, pp. 402–409.

[13] D. B. Arnold, M. Sankur, R. Dobbe, K. Brady, D. S. Callaway, and A. Von Meier, "Optimal dispatch of reactive power for voltage regulation and balancing in unbalanced distribution systems," in *2016 IEEE Power and Energy Society General Meeting (PESGM)*. IEEE, 2016, pp. 1–5.

[14] J. A. Taylor, *Convex optimization of power systems*. Cambridge University Press, 2015.

[15] L. Gan, N. Li, U. Topcu, and S. H. Low, "Exact convex relaxation of optimal power flow in radial networks," *IEEE Transactions on Automatic Control*, vol. 60, no. 1, pp. 72–87, 2015.

[16] S. Huang, Q. Wu, J. Wang, and H. Zhao, "A sufficient condition on convex relaxation of AC optimal power flow in distribution networks," *IEEE Transactions on Power Systems*, vol. 32, no. 2, pp. 1359–1368, 2017.

[17] D. Molzahn and L. A. Roald, "Grid-aware versus grid-agnostic distribution system control: A method for certifying engineering constraint satisfaction," in *Hawaii International Conference on System Sciences*, 2019.

[18] D. Lee, H. D. Nguyen, K. Dvijotham, and K. Turitsyn, "Convex restriction of power flow feasibility sets," *IEEE Transactions on Control of Network Systems*, vol. 6, no. 3, pp. 1235–1245, 2019.

[19] D. Lee, K. Turitsyn, D. K. Molzahn, and L. Roald, "Feasible path identification in optimal power flow with sequential convex restriction," *IEEE Transactions on Power Systems*, 2020.

[20] M. Nick, R. Cherkaoui, J.-Y. Le Boudec, and M. Paolone, "An exact convex formulation of the optimal power flow in radial distribution networks including transverse components," *IEEE Transactions on Automatic Control*, vol. 63, no. 3, pp. 682–697, 2017.

[21] S. C. Ross and J. L. Mathieu, "A method for ensuring a load aggregator's power deviations are safe for distribution networks," *Electric Power Systems Research*, vol. 189, p. 106781, 2020.

[22] J.-S. Chang and C.-K. Yap, "A polynomial solution for the potato-peeling problem," *Discrete & Computational Geometry*, vol. 1, no. 2, pp. 155–182, 1986.

[23] N. Nazir, P. Racherla, and M. Almassalkhi, "Optimal multi-period dispatch of distributed energy resources in unbalanced distribution feeders," *IEEE Transactions on Power Systems*, vol. 35, no. 4, pp. 2683–2692, 2020.

[24] E. Dall'Anese, S. S. Guggilam, A. Simonetto, Y. C. Chen, and S. V. Dhople, "Optimal regulation of virtual power plants," *IEEE Transactions on Power Systems*, vol. 33, no. 2, pp. 1868–1881, 2017.

[25] N. Nazir and M. Almassalkhi, "Voltage positioning using co-optimization of controllable grid assets in radial networks," *preprint arXiv:1911.00338*, 2020.

[26] R. Heidari, M. M. Seron, and J. H. Braslavsky, "Non-local approximation of power flow equations with guaranteed error bounds," in *Control Conference (ANZCC), 2017 Australian and New Zealand*, 2017, pp. 83–88.

[27] R. D. Zimmerman, C. E. Murillo-Sánchez, and R. J. Thomas, "Matpower: Steady-state operations, planning, and analysis tools for power systems research and education," *IEEE Transactions on power systems*, vol. 26, no. 1, pp. 12–19, 2011.

[28] I. J. Pérez-Arriaga, J. D. Jenkins, and C. Batlle, "A regulatory framework for an evolving electricity sector: Highlights of the MIT utility of the future study," *Economics of Energy & Environmental Policy*, vol. 0, no. Number 1, 2017.

[29] M. Rosenlicht, *Introduction to analysis*. Courier Corporation, 1986.

[30] K. A. Horowitz, A. Jain, F. Ding, B. Mather, and B. Palmintier, "A techno-economic comparison of traditional upgrades, volt-var controls, and coordinated distributed energy resource management systems for integration of distributed photovoltaic resources," *International Journal of Electrical Power & Energy Systems*, vol. 123, p. 106222, 2020.

[31] K. Baker, A. Bernstein, E. Dall'Anese, and C. Zhao, "Network-cognizant voltage droop control for distribution grids," *IEEE Transactions on Power Systems*, vol. 33, no. 2, pp. 2098–2108, 2018.

[32] H.-D. Chiang and M. E. Baran, "On the existence and uniqueness of load flow solution for radial distribution power networks," *IEEE Transactions on Circuits and Systems*, vol. 37, no. 3, pp. 410–416, 1990.

[33] D. K. Molzahn, B. C. Lesieutre, and C. L. DeMarco, "Investigation of non-zero duality gap solutions to a semidefinite relaxation of the optimal power flow problem," in *2014 47th Hawaii International Conference on System Sciences*. IEEE, 2014, pp. 2325–2334.

[34] C. Wang, A. Bernstein, J. Le Boudec, and M. Paolone, "Explicit conditions on existence and uniqueness of load-flow solutions in distribution networks," *IEEE Transactions on Smart Grid*, vol. 9, no. 2, pp. 953–962, 2018.

[35] A. Bernstein, C. Wang, E. Dall'Anese, J.-Y. Le Boudec, and C. Zhao, "Load flow in multiphase distribution networks: Existence, uniqueness, non-singularity and linear models," *IEEE Transactions on Power Systems*, vol. 33, no. 6, pp. 5832–5843, 2018.

[36] B. Cui and X. A. Sun, "Solvability of power flow equations through existence and uniqueness of complex fixed point," *arXiv preprint arXiv:1904.08855*, 2019.

[37] "IEEE standard for interconnection and interoperability of distributed energy resources with associated electric power systems interfaces," *IEEE Std 1547-2018 (Revision of IEEE Std 1547-2003)*, April 2018.